Attenuation of Allergic Contact Dermatitis Through the Endocannabinoid System

Meliha Karsak,[1]* Evelyn Gaffal,[2]* Rahul Date,[1] Lihua Wang-Eckhardt,[3] Jennifer Rehnelt,[1] Stefania Petrosino,[4] Katarzyna Starowicz,[4] Regina Steuder,[2] Eberhard Schlicker,[5] Benjamin Cravatt,[6] Raphael Mechoulam,[7] Reinhard Buettner,[8] Sabine Werner,[9] Vincenzo Di Marzo,[4] Thomas Tüting,[2]† Andreas Zimmer[1]†

Allergic contact dermatitis affects about 5% of men and 11% of women in industrialized countries and is one of the leading causes for occupational diseases. In an animal model for cutaneous contact hypersensitivity, we show that mice lacking both known cannabinoid receptors display exacerbated allergic inflammation. In contrast, fatty acid amide hydrolase–deficient mice, which have increased levels of the endocannabinoid anandamide, displayed reduced allergic responses in the skin. Cannabinoid receptor antagonists exacerbated allergic inflammation, whereas receptor agonists attenuated inflammation. These results demonstrate a protective role of the endocannabinoid system in contact allergy in the skin and suggest a target for therapeutic intervention.

Allergic contact dermatitis is characterized by a loss of immunological tolerance toward small allergenic molecules (haptens). The allergen or hapten first penetrates the epidermis and is taken up by skin dendritic cells, which migrate to the draining lymph nodes and present haptenated peptide or major histocompatibility complexes (MHC) to naïve antigen-specific T lymphocytes. Upon repeated allergen contact, an inflammatory response is elicited by the recruitment of antigen-specific effector T cells to the skin and the subsequent production of inflammatory cytokines and chemokines (*1*). Cannabinoid receptors CB1 and CB2 are heterotrimeric GTP-binding protein (G protein)–coupled receptors, which are activated by the cannabinoid Δ^9-tetrahydrocannabinol (Δ^9-THC), as well as by endocannabinoids such as arachidonoylethanolamide (anandamide or AEA) or 2-arachidonoylglycerol (2-AG) (*2*). Both cannabinoid receptors are present on keratinocytes in the epidermis, which also express enzymes involved in the synthesis and degradation of endocannabinoids (*3*, *4*).

Although nickel-containing ear tags are generally well tolerated by individuals in our mouse colony (*5*), we observed that mice lacking both cannabinoid CB1 and CB2 receptors [CB1 receptor–deficient ($Cnr1^{-/-}$) and CB2 receptor–deficient ($Cnr2^{-/-}$) mice] (*6*, *7*) frequently scratch their ear tags, leading to severe ulcerations in the head and neck regions (Fig. 1, A and B, and fig. S1). Because localized necrotic lesions initially developed around the ear tag, we first considered that impaired wound healing might be the potential primary cause for the skin lesions. However, experiments to test the wound healing ability revealed no measurable difference between wild-type (WT) and $Cnr1^{-/-}/Cnr2^{-/-}$ double-knockout (DKO) mice (*5*, *8*) (fig. S2). We also noted that skin ulcerations appeared to be particularly prominent in mice with tags containing high nickel content (65 to 70%). In these cases, skin ulcerations were observed in 88 out of 304 $Cnr1^{-/-}/Cnr2^{-/-}$ DKO mice (29%), but were not observed in single $Cnr1^{-/-}$ or $Cnr2^{-/-}$ knockouts or in any other mouse strain. Furthermore, no ulcerations were noted in mice with pure brass tags (fig. S1). Subsequent histopathological analyses of ulcerated ear tissue revealed intense infiltration of mast cells in close proximity to the ulcers (Fig. 1, C and D), suggesting that an allergic reaction might be involved in the pathology seen in $Cnr1^{-/-}/Cnr2^{-/-}$ DKO mice. Consistently, the regional preauricular and submental lymph nodes (Fig. 1, E and F) were swollen, reaching a diameter of 51 ± 2.4 mm in comparison with 20.5 ± 1.9 mm in healthy $Cnr1^{-/-}/Cnr2^{-/-}$ mice, as a result of mixed follicular and interfollicular lymphatic hyperplasia.

We therefore considered the possibility that an increase in allergic responses might exist in knockout (KO) mice. To test this hypothesis, we evaluated cutaneous contact hypersensitivity (CHS) in $Cnr1^{-/-}/Cnr2^{-/-}$ animals using the obligate contact allergen 2,4-dinitrofluorobenzene (DNFB), which generates a specific cutaneous T cell–mediated allergic response upon repeated allergen contact (*9*). A marked increase in allergic

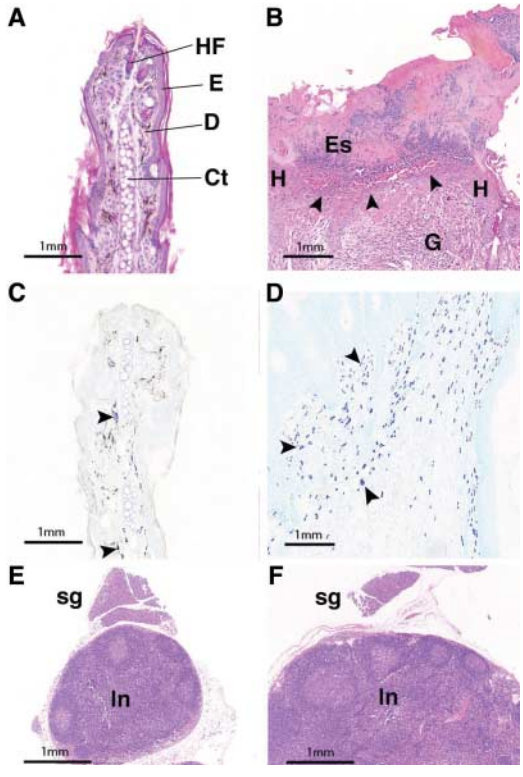

Fig. 1. Histological views of $Cnr1^{-/-}/Cnr2^{-/-}$ mouse ears. Clips with high nickel content cause chronic ear ulceration in $Cnr1^{-/-}/Cnr2^{-/-}$ mice (fig. S1). (**A**) Hematoxylin and eosin (H&E)–stained sections of ear tissue from healthy $Cnr1^{-/-}/Cnr2^{-/-}$ mice with normal size and histology. Ct, cartilage; D, dermis; E, epidermis; HF, hair follicle. (**B**) H&E–stained sections of ulcerated ear tissue from $Cnr1^{-/-}/Cnr2^{-/-}$ mice carrying nickel ear tags. Arrowheads point to keratinocytes on the re-epithelized body of the wound. The eschar (Es), the strong hyperproliferative epithelium (H), and the granulation tissue (G) are indicated. (**C**) Toluidine blue–stained sections of ear tissue from healthy $Cnr1^{-/-}/Cnr2^{-/-}$ mice showing few metachromatic mast cells (arrowheads). (**D**) Toluidine blue–stained sections of ulcerated ear tissue from $Cnr1^{-/-}/Cnr2^{-/-}$ mice carrying nickel tags with intense infiltration of mast cells (arrowheads). (**E**) H&E–stained sections of lymph nodes from healthy $Cnr1^{-/-}/Cnr2^{-/-}$ mice. ln, lymph node; sg, salivary gland. (**F**) H&E–stained sections of lymph nodes from $Cnr1^{-/-}/Cnr2^{-/-}$ mice carrying nickel ear tags with reactive enlargement and lymphadenitis of preauricular lymph nodes. The preauricular salivary glands located next to the lymph nodes are the same size in $Cnr1^{-/-}/Cnr2^{-/-}$ mice without (E) and with (F) ear ulceration and serve as an internal standard.

[1]Department of Molecular Psychiatry, University of Bonn, Germany. [2]Laboratory of Experimental Dermatology, Department of Dermatology, University of Bonn, Germany. [3]Life & Brain GmbH, Bonn, Germany. [4]Endocannabinoid Research Group, Institute of Biomolecular Chemistry, Consiglio Nazionale delle Ricerche, Pozzuoli (Napoli), Italy. [5]Institute of Pharmacology and Toxicology, University of Bonn, Germany. [6]The Skaggs Institute for Chemical Biology and Departments of Cell Biology and Chemistry, The Scripps Research Institute, La Jolla, CA, USA. [7]Department of Medicinal Chemistry and Natural Products, The Hebrew University of Jerusalem, Israel. [8]Department of Pathology, University of Bonn, Germany. [9]Institute of Cell Biology, Eidgenössische Technische Hochschule, Zurich, Switzerland.

*These authors contributed equally to this work.
†To whom correspondence should be addressed. E-mail: a.zimmer@uni-bonn.de (A.Z.); thomas.tueting@ukb.uni-bonn.de (T.T.)

responses was apparent in $Cnr1^{-/-}/Cnr2^{-/-}$ mice as compared with WT controls (Fig. 2A). The difference was particularly prominent 48 hours after the second and the third DNFB challenge. Infiltration of the skin with Gr-1^{+} granulocytes was increased in the ears of DNFB-exposed $Cnr1^{-/-}/Cnr2^{-/-}$ mice, as compared with WT animals (fig. S3), and correlated with a higher myeloperoxidase activity, which is indicative of enhanced neutrophil recruitment (*10*, *11*). Furthermore, we found an increased number of MHC II^{+} antigen-presenting cells in $Cnr1^{-/-}/Cnr2^{-/-}$ mice. Upon examination of mice with a single deletion of either CB1 or CB2 receptors, we observed a similarly pronounced increase of allergic ear swelling (Fig. 2B), suggesting a nonredundant role for each cannabinoid receptor in the allergic response to DNFB. This finding would also suggest that the response to the milder stimulus originating from the nickel ear tag was only detectable in mice lacking both receptors.

In order to obtain independent evidence for a role of the CB1 and CB2 receptors in the regulation of CHS, we examined WT mice after administration of the CB1 receptor antagonist SR141716A (Rimonabant) and the CB2 receptor antagonist SR144528, respectively. After the induction of CHS, animals received three injections of the corresponding antagonist 30 min before and after each challenge. In these cases, ear swelling was significantly increased in treated mice as compared with control mice (Fig. 2C), further supporting the role of both receptors in CHS. In contrast, however, acute oral or topical administration of the CB2 receptor antagonists appeared to ameliorate inflammatory skin responses (*12*, *13*), thus suggesting that CB2 antagonism may be initially beneficial but detrimental upon chronic blockade.

To explore this issue more carefully, we investigated the synthesis of endogenous cannabinoids and the expression of cannabinoid receptors during experimental contact allergy studies. After DNFB treatment, the levels of 2-AG increased in the DNFB-treated ears of WT controls and to an even larger extent in the ears of $Cnr1^{-/-}/Cnr2^{-/-}$ mice (Fig. 3A), whereas AEA production was strongly induced in both genotypes. Endocannabinoids may have been overproduced in KO animals as a result of the lack of communication between receptors and ligands (*14*) or as a further consequence of the exacerbated allergic response. Keratinocytes are known to express CB1 receptors (*4*), although the expression of CB2 on these

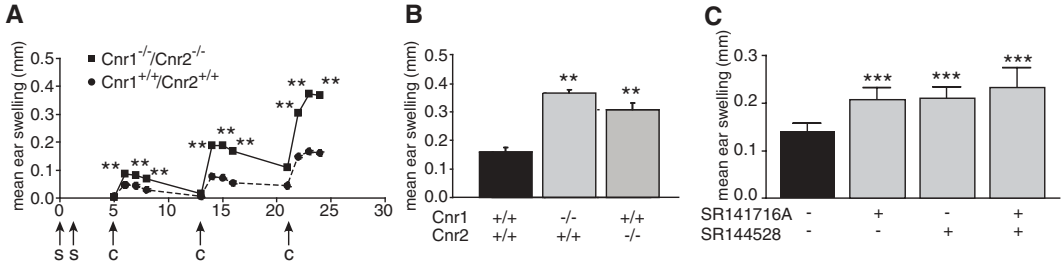

Fig. 2. Contact allergy in cannabinoid receptor–deficient mice. (**A**) $Cnr1^{-/-}/Cnr2^{-/-}$ and $Cnr1^{+/+}/Cnr2^{+/+}$ mice were sensitized (indicated by "s") with DNFB on the shaved abdomen. On day 5, mice were challenged (indicated by "c") with DNFB on the right ear. A second and third challenge was performed on day 13 and 21. Shown is the mean ear swelling over time ± SEM of a representative experiment with nine mice per group. Statistical significance was evaluated with the Wilcoxon-Mann-Whitney two-sample test (**$P < 0.01$). This experiment was independently repeated four times with similar results. (**B**) $Cnr1^{-/-}/Cnr2^{+/+}$, $Cnr1^{+/+}/Cnr2^{-/-}$, and $Cnr1^{+/+}/Cnr2^{+/+}$ mice were sensitized as described in (A). Ear swelling 48 hours after the third challenge of a representative experiment with eight mice per group is shown. Similar results were obtained in four independent experiments with a total of 23 mice (**$P < 0.01$). (**C**) Contact allergic response in C57BL/6J mice after treatment with the indicated CB receptor antagonists. Ear swelling 48 hours after the second challenge of a representative experiment with 10 mice per group is shown. Similar results were obtained in four independent experiments with a total of 25 mice (***$P < 0.001$). Error bars in (B) and (C) indicate SEM.

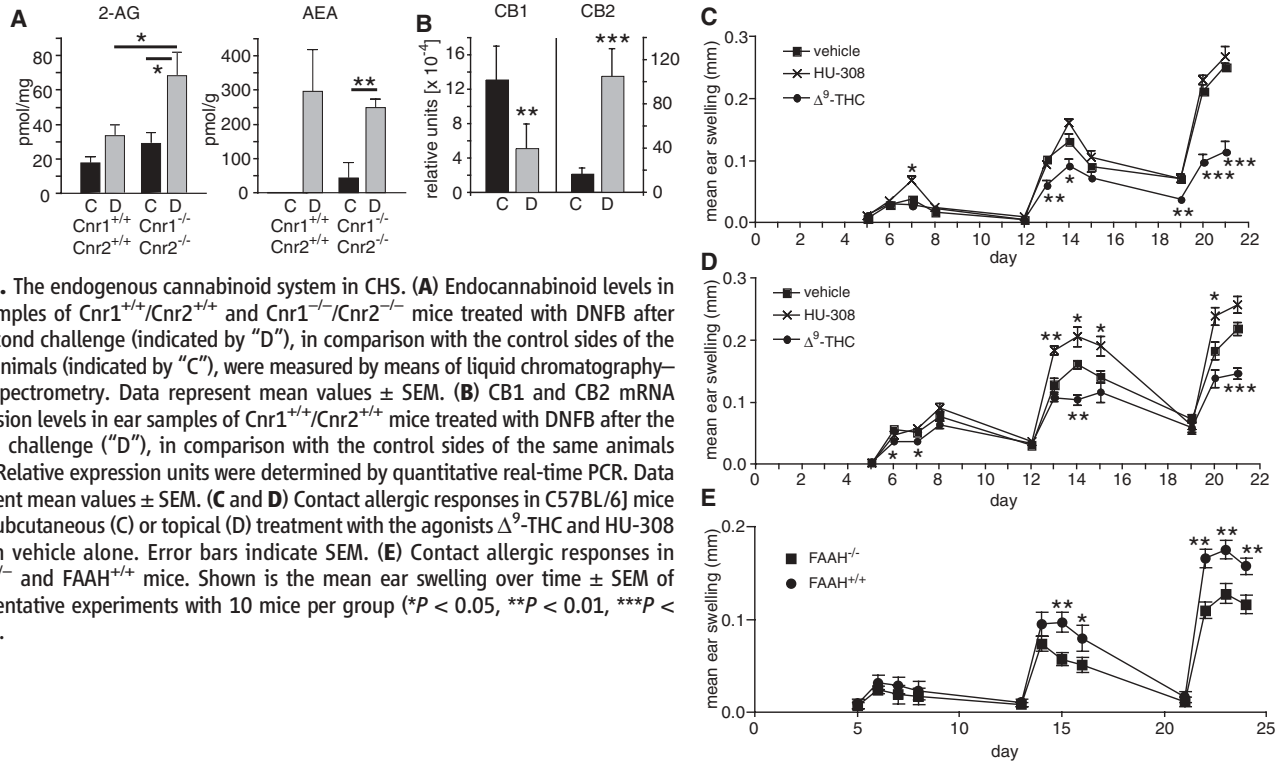

Fig. 3. The endogenous cannabinoid system in CHS. (**A**) Endocannabinoid levels in ear samples of $Cnr1^{+/+}/Cnr2^{+/+}$ and $Cnr1^{-/-}/Cnr2^{-/-}$ mice treated with DNFB after the second challenge (indicated by "D"), in comparison with the control sides of the same animals (indicated by "C"), were measured by means of liquid chromatography–mass spectrometry. Data represent mean values ± SEM. (**B**) CB1 and CB2 mRNA expression levels in ear samples of $Cnr1^{+/+}/Cnr2^{+/+}$ mice treated with DNFB after the second challenge ("D"), in comparison with the control sides of the same animals ("C"). Relative expression units were determined by quantitative real-time PCR. Data represent mean values ± SEM. (**C** and **D**) Contact allergic responses in C57BL/6J mice after subcutaneous (C) or topical (D) treatment with the agonists Δ^9-THC and HU-308 or with vehicle alone. Error bars indicate SEM. (**E**) Contact allergic responses in $FAAH^{-/-}$ and $FAAH^{+/+}$ mice. Shown is the mean ear swelling over time ± SEM of representative experiments with 10 mice per group (*$P < 0.05$, **$P < 0.01$, ***$P < 0.001$).

cells has been debated (*3*, *12*, *15*). We could identify both receptor mRNAs in human HaCat keratinocytes (fig. S4). CB1 receptor mRNA was down-regulated in HaCat cells that had been stimulated for 24 hours with polyinosinic-polycytidylic acid and also in DNFB-exposed ears, whereas CB2 mRNA and protein expression was up-regulated in both cases (Fig. 3B and fig. S4). Taken together, these findings indicate that DNFB-induced CHS caused an activation of the endocannabinoid system in the skin and imbalanced expression of both receptors.

Because our data indicate that activation of the endocannabinoid system may function to dampen the CHS response, we considered the possibility that administration of cannabinoids such as Δ^9-THC might attenuate CHS in WT animals. Therefore, after CHS was induced, we injected mice with Δ^9-THC (5 mg per kilogram of body weight, administered subcutaneously) 30 min before, as well as 24 and 48 hours after, DNFB challenge. Indeed, Δ^9-THC significantly decreased ear swelling (Fig. 3C) and reduced the recruitment of Gr-1^+ granulocytes in comparison with swelling and granulocyte recruitment in untreated mice [vehicle: 483 ± 62 Gr-1^+ cells per high power field (HPF) versus 200 ± 50 Gr-1^+ cells per HPF in subcutaneous THC treatment]. A similar therapeutic effect of Δ^9-THC was observed after topical application of 30 μg of Δ^9-THC 30 min before, as well as 24 and 48 hours after, DNFB administration (Fig. 3D). In contrast, the CB2-specific agonist HU-308 either showed no efficacy or even increased the allergic response after subcutaneous or topical application (Fig. 3, C and D) (*13*). It has recently been shown that leukocyte chemotaxis is inhibited by the CB2 receptor inverse agonist *N*-[1(*S*)-[4-[[4-methoxy-2-[(4-methoxyphenyl)sulfonyl]phenyl]-sulfonyl]phenyl]ethyl]methanesulfonamide (Sch. 336) and, thus, HU-308 administration to the inflamed ear may have further increased leukocyte infiltration (*16*).

Because endocannabinoid levels were regulated in DNFB-treated ears and Δ^9-THC had a beneficial effect on CHS, we asked whether mice having higher endocannabinoid levels would show altered allergic responses after DNFB treatment. Therefore, we analyzed the allergic reaction in mice lacking the enzyme fatty acid amide hydrolase (FAAH), which have augmented anandamide levels (*17*). As shown in Fig. 3E, we found a significantly decreased allergic response in FAAH KO mice after the second and third DNFB challenge when compared with the response in WT mice. Similar to our results, mice with only peripherally elevated fatty acid amides showed a reduced inflammation in the carrageenan foot-pad model (*18*). All data indicate that the anti-inflammatory responses were peripheral, rather than central, and that FAAH inhibitors are a potential therapeutic approach for inflammation (and a potentially useful alternative to direct CB1/CB2 agonists).

In order to gain insight into the molecular mechanism that may contribute to the increased magnitude of CHS in cannabinoid receptor–deficient mice, we performed a series of microarray experiments with RNA isolated from DNFB-treated ears of Cnr$1^{-/-}$/Cnr$2^{-/-}$ and Cnr$1^{+/+}$/Cnr$2^{+/+}$ mice, as well as from the untreated ears of control mice. In all, 830 probe sets were differentially expressed between control and DNFB-treated ears, of which 674 were up-regulated and only 156 were down-regulated. We grouped the probe sets by using gene ontology (GO) annotation (*19*, *20*) (Fig. 4A). Immune-related probe sets represented the largest group of differentially expressed genes (40 down-regulated and 117 up-regulated probe sets). Notably, large numbers of chemokine C-C and C-X-C motif ligands (*21*) and receptors were found in the up-regulated group (table S1) and represented 22% of the immune-related probe sets (table S2). Fifty-four genes were differentially expressed in DNFB-treated whole-ear specimens of Cnr$1^{+/+}$/Cnr$2^{+/+}$ mice versus those of Cnr$1^{-/-}$/Cnr$2^{-/-}$ mice (fig. S5). The only chemokine gene transcript in this group was monocyte chemotactic protein 2 (MCP-2)/chemokine (C-C motif) ligand 8 (CCL8). Using real-time reverse transcription polymerase chain reaction (RT-PCR) and in situ hybridization, we confirmed the differential expression of MCP-2/CCL8 mRNA in keratinocytes (Fig. 4, B and C). Further in vitro experiments showed dynamic regulation of MCP-2/CCL8 production in activated keratinocytes through cannabinoid agonists (fig. S6). MCP-2/CCL8 is a member of the MCP family, which has been shown to play a major role in the recruitment of macrophages, activated lymphocytes, and mast cells into inflammatory sites (*22*, *23*). Taken together, our results suggest that the endocannabinoid system regulates allergic inflammation through a modulation of the chemokine system.

The observation that the endocannabinoid system is activated in a model of CHS, together with the fact that genetic deletion or pharmacologic blockade of CB receptors enhanced contact allergic inflammation, whereas stimulation of CB receptors reduced such inflammation, strongly suggests that the endocannabinoid system serves to attenuate the inflammatory re-

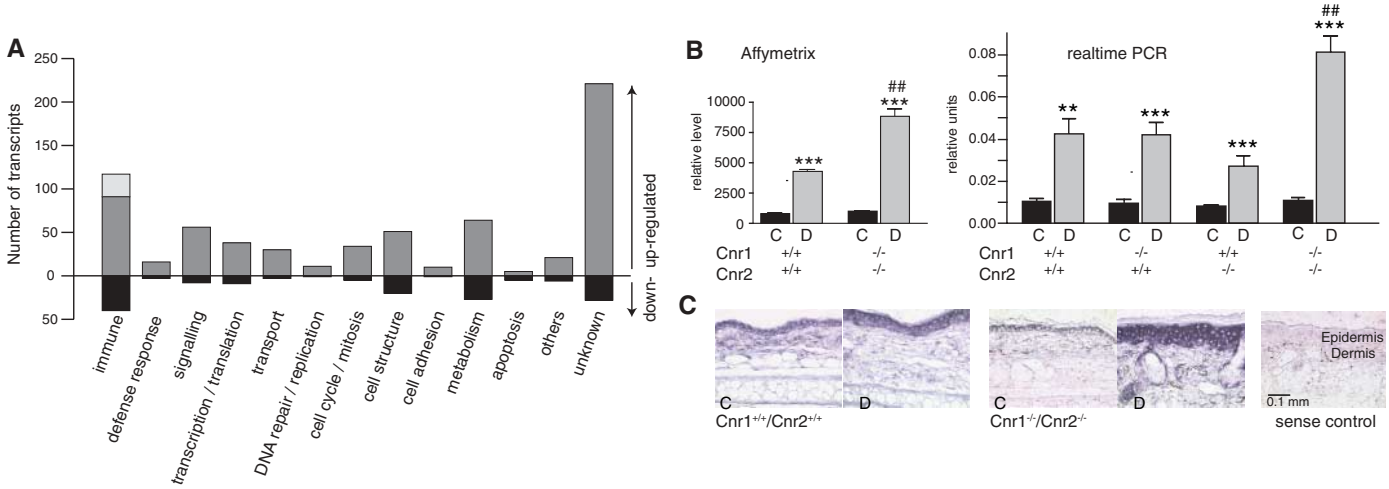

Fig. 4. Gene expression analysis. (**A**) Microarray analysis of ear samples of Cnr$1^{+/+}$/Cnr$2^{+/+}$ and Cnr$1^{-/-}$/Cnr$2^{-/-}$ mice treated with DNFB 48 hours after the second challenge ("D") in comparison with the control sides of the same animals ("C") revealed 674 up-regulated and 156 down-regulated probe sets in response to the treatment. Grouping was performed by GO annotation. Chemokine C-C motif and C-X-C motif ligands and receptors in the up-regulated group are presented in light gray in the column of immune-related genes. (**B**) Transcripts for the chemokine MCP-2/CCL8 in DNFB-treated ears of Cnr$1^{+/+}$/Cnr$2^{+/+}$ and Cnr$1^{-/-}$/Cnr$2^{-/-}$ mice resulting from microarray expression study (left panel) and real-time RT-PCR quantification (right panel). Shown are representative results of three independent experiments (**P < 0.01, ##P < 0.01, ***P < 0.001). Error bars indicate SEM. (**C**) In situ hybridization with the use of a digoxigenin-labeled probe for MCP-2/CCL8 in ear tissue of DNFB-treated and control ears from Cnr$1^{+/+}$/Cnr$2^{+/+}$ and Cnr$1^{-/-}$/Cnr$2^{-/-}$ mice. The sense probe showed no staining.

sponse in cutaneous CHS. The finding that topical application of Δ^9-THC reduced allergic inflammation points to the promising potential of developing pharmacological treatments (*24*) with the use of selective CB receptor agonists or FAAH inhibitors.

References and Notes

1. S. Grabbe, T. Schwarz, *Immunol. Today* **19**, 37 (1998).
2. T. Bisogno, A. Ligresti, V. Di Marzo, *Pharmacol. Biochem. Behav.* **81**, 224 (2005).
3. M. M. Ibrahim *et al.*, *Proc. Natl. Acad. Sci. U.S.A.* **102**, 3093 (2005).
4. M. Maccarrone *et al.*, *J. Biol. Chem.* **278**, 33896 (2003).
5. Materials and methods are available as supporting material on *Science* Online.
6. A. Zimmer, A. M. Zimmer, A. G. Hohmann, M. Herkenham, T. I. Bonner, *Proc. Natl. Acad. Sci. U.S.A.* **96**, 5780 (1999).
7. N. E. Buckley *et al.*, *Eur. J. Pharmacol.* **396**, 141 (2000).
8. S. Werner *et al.*, *Science* **266**, 819 (1994).
9. J. Knop, R. Stremmer, C. Neumann, E. De Maeyer, E. Macher, *Nature* **296**, 757 (1982).
10. R. I. Lehrer, J. Hanifin, M. J. Cline, *Nature* **223**, 78 (1969).
11. C. Nathan, *Nat. Rev. Immunol.* **6**, 173 (2006).
12. S. Oka *et al.*, *J. Immunol.* **177**, 8796 (2006).
13. Y. Ueda, N. Miyagawa, T. Matsui, T. Kaya, H. Iwamura, *Eur. J. Pharmacol.* **520**, 164 (2005).
14. V. Di Marzo *et al.*, *J. Neurochem.* **75**, 2434 (2000).
15. S. Stander, M. Schmelz, D. Metze, T. Luger, R. Rukwied, *J. Dermatol. Sci.* **38**, 177 (2005).
16. C. A. Lunn *et al.*, *J. Pharmacol. Exp. Ther.* **316**, 780 (2006).
17. B. F. Cravatt *et al.*, *Proc. Natl. Acad. Sci. U.S.A.* **98**, 9371 (2001).
18. B. F. Cravatt *et al.*, *Proc. Natl. Acad. Sci. U.S.A.* **101**, 10821 (2004).
19. J. S. Lee, G. Katari, R. Sachidanandam, *BMC Bioinformat.* **6**, 189 (2005).
20. M. Ashburner *et al.*, *Nat. Genet.* **25**, 25 (2000).
21. M. F. Bachmann, M. Kopf, B. J. Marsland, *Nat. Rev. Immunol.* **6**, 159 (2006).
22. A. de Paulis *et al.*, *Int. Arch. Allergy Immunol.* **124**, 146 (2001).
23. D. D. Taub *et al.*, *J. Clin. Invest.* **95**, 1370 (1995).
24. T. W. Klein, *Nat. Rev. Immunol.* **5**, 400 (2005).

25. This work was supported by grants from the Deutsche *Forschungsgemeinschaft* [SFB645 and GRK804 (to M.K. and A.Z.) and Tu90/5-1 (to T.T.)], by a Bonfor stipend to E.G., and a grant from Epitech S.r.l. to V.D.M. We thank M. Krampert for her help in wound healing experiments, L. Cristino for her help with immunohistochemistry, and J. Essig, A. Zimmer, E. Erxlebe, and I. Heim for technical assistance.

Supporting Online Material

www.sciencemag.org/cgi/content/full/316/5830/1494/DC1
Materials and Methods
Figs. S1 to S6
Tables S1 and S2
References

8 March 2007; accepted 4 May 2007
10.1126/science.1142265

Genome-Wide Mapping of in Vivo Protein-DNA Interactions

David S. Johnson,[1]* Ali Mortazavi,[2]* Richard M. Myers,[1]† Barbara Wold[2,3]†

In vivo protein-DNA interactions connect each transcription factor with its direct targets to form a gene network scaffold. To map these protein-DNA interactions comprehensively across entire mammalian genomes, we developed a large-scale chromatin immunoprecipitation assay (ChIPSeq) based on direct ultrahigh-throughput DNA sequencing. This sequence census method was then used to map in vivo binding of the neuron-restrictive silencer factor (NRSF; also known as REST, for repressor element–1 silencing transcription factor) to 1946 locations in the human genome. The data display sharp resolution of binding position [±50 base pairs (bp)], which facilitated our finding motifs and allowed us to identify noncanonical NRSF-binding motifs. These ChIPSeq data also have high sensitivity and specificity [ROC (receiver operator characteristic) area ≥ 0.96] and statistical confidence ($P < 10^{-4}$), properties that were important for inferring new candidate interactions. These include key transcription factors in the gene network that regulates pancreatic islet cell development.

Although much is known about transcription factor binding and action at specific genes, far less is known about the composition and function of entire factor-DNA interactomes, especially for organisms with large genomes. Now that human, mouse, and other large genomes have been sequenced, it is possible, in principle, to measure how any transcription factor is deployed across the entire genome for a given cell type and physiological condition. Such measurements are important for systems-level studies because they provide a global map of candidate gene network input connections. These direct physical interactions between transcription factors or cofactors and the chromosome can be detected by chromatin immunoprecipitation (ChIP) (*1*). In ChIP experiments, an immune reagent specific for a DNA binding factor is used to enrich target DNA sites to which the factor was bound in the living cell. The enriched DNA sites are then identified and quantified.

For the gigabase-size genomes of vertebrates, it has been difficult to make ChIP measurements that combine high accuracy, whole-genome completeness, and high binding-site resolution. These data-quality and depth issues dictate whether primary gene network structure can be inferred with reasonable certainty and comprehensiveness, and how effectively the data can be used to discover binding-site motifs by computational methods. For these purposes, statistical robustness, sampling depth across the genome, absolute signal and signal-to-noise ratio must be good enough to detect nearly all in vivo binding locations for a regulator with minimal inclusion of false-positives. A further challenge in genomes large or small is to map factor-binding sites with high positional resolution. In addition to making computational discovery of binding motifs feasible, this dictates the quality of regulatory site annotation relative to other gene anatomy landmarks, such as transcription start sites, enhancers, introns and exons, and conserved noncoding features (*2*). Finally, if high-quality protein-DNA interactome measurements can be performed routinely and at reasonable cost, it will open the way to detailed studies of interactome dynamics in response to specific signaling stimuli or genetic mutations. To address these issues, we turned to ultrahigh-throughput DNA sequencing to gain sampling power and applied size selection on immuno-enriched DNA to enhance positional resolution.

The ChIPSeq assay shown here differs from other large-scale ChIP methods such as ChIPArray, also called ChIPchip (*1*); ChIPSAGE (SACO) (*3*); or ChIPPet (*4*) in design, data produced, and cost. The design is simple (Fig. 1A) and, unlike SACO or ChIPPet, it involves no plasmid library construction. Unlike microarray assays, the vast majority of single-copy sites in the genome is accessible for ChIPSeq assay (*5*), rather than a subset selected to be array features. For example, to sample with similar completeness by an Affymetrix-style microarray design, a nucleotide-by-nucleotide sliding window design of roughly 1 billion features per array would be needed for the nonrepeat portion of the human genome. In addition, ChIPSeq counts sequences and so avoids constraints imposed by array hybridization chemistry, such as base composition constraints related to T_m, the temperature at which 50% of double-stranded DNA or DNA-RNA hybrids is denatured; cross-hybridization; and secondary structure interference. Finally, ChIPSeq is feasible for any sequenced genome, rather than being restricted to species for which whole-genome tiling arrays have been produced.

ChIPSeq illustrates the power of new sequencing platforms, such as those from Solexa/Illumina and 454, to perform sequence census counting assays. The generic task in these applications is to identify and quantify the molecular

[1]Department of Genetics, Stanford University School of Medicine, Stanford, CA, 94305–5120, USA. [2]Biology Division, California Institute of Technology, Pasadena, CA 91125, USA. [3]California Institute of Technology Beckman Institute, Pasadena, CA 91125, USA.

*These authors contributed equally to this work.
†To whom correspondence should be addressed. E-mail: woldb@its.caltech.edu (B.W.); myers@shgc.stanford.edu (R.M.M.)